A Generalized case of Electromagnetic Scattering from a finite number of Ferromagnetic cylinders

Tarun Kumar[1]*, **Natarajan Kalyanasundaram**[1], **Bhaurao K. Lande**[2],

[1]JayPee Institute of Information Technology, A-10, Sector 62, Noida, Uttar Pradesh 201307, India
[2]Swami Rama Himalayan University, Jolly Grant, Dehradun, Uttarakhand 248140, India
*corresponding author, E-mail: tk.parashar@gmail.com

Abstract

A generalized solution of the scattering problem from an array containing a finite number of axially magnetized ferromagnetic cylinders of infinite length placed in free space is presented in this paper. The analysis is carried out by matching the tangential boundary conditions at the surface of each cylinder to find the unknown expansion coefficients of the scattered field. Planar arrays consist of a finite number of ferromagnetic microwires are considered to obtain the numerical results for TM_z and TE_z polarizations in terms of the variation in scattered field components of the near field and scattering cross section (SCS) with respect to angle of incidence, radius of microwires, spacing among the microwires and operating frequency. For validation purpose, numerical results of the proposed analysis specialized for the case of single microwire and normal incidence for TM_z polarization are compared with the results available in the literature for the specialized case and both are found to be matched completely.

1. Introduction

Wire-based metamaterials(MTMs) have become a key research area in the recent past[1, 2, 3]. Recently, Ferrites are reported to be used for designing wire-based double negative(DNG) metamaterials due to the occurrence of a well known phenomenon in ferromagnetic materials which is called ferromagnetic resonance(FMR) inside the ferrite medium due to which the real part of permeability $Re[\mu_e]$ of the ferrite medium becomes negative(see in Fig.(1)) beyond FMR frequency[4, 5, 6, 7]. Study of the scattering properties of a ferrite grid structure plays a key role in the designing of wire-based metamaterials(MTMs).Scattering from single ferrite cylinder for normal incidence case as well as for the generalized case has been investigated by many authors[4, 5, 6, 7]. The problem of two dimensional scattering from an array of ferrite,conducting and dielectric cylinders has also been studied for many years using various techniques[8, 10, 11, 12, 13] among which the boundary value type solution is found to be very accurate[11]. Recently, a generalized case of scattering from a grid containing an infinite number of ferromagnetic microwires has been reported in[9]. In real time situation, scattering from finite number of microwires may be of more practical in-

terest. Okomoto in [14], has derived a solution for electromagnetic scattering from plural gyromagnetic homogeneous circular cylinders for an obliquely incident uniform plane wave by assuming auxiliary electric and magnetic current sources and using reciprocity theorem. But the approach in [14] seems to be more complex because it rederives the expressions for the inside fields of the gyromagnetic medium. As the generalized expressions for the inside fields of the ferrite cylinders are already available in literature[6, 7], the exact solution for the problem of scattering from finite number of ferrite cylinders can be easily obtained with less efforts by using tangential boundary conditions at the surface of each cylinder. In this paper, an boundary value type solution is obtained in a similar manner as in [9] for the generalized case of scattering from finite number of ferromagnetic cylinders placed in free space and illuminated by a uniform plane wave. The solution is obtained by calculating the unknown expansion coefficients of the scattered field by matching the tangential boundary conditions at the surface of each microwire. Graf's Addition theorem is used to suitably transform the scattered field from one coordinate system to another. As a numerical example, the solution obtained hereby, is applied to a planar array consist of a finite number of microwires. Sample results are expressed in terms of the near field components of the scattered field and Scattering cross section(SCS) for TM_z and TE_z polarizations. In order to validate the proposed method of analysis, numerical results of scattering field coefficient obtained by the proposed method for the specialized case of single microwire and normal incidence for for TM_z polarization are compared with the result available in [4].

2. Formulation of The Scattered Field

Tensorial nature of the permeability of ferrite medium arises due to the interaction of applied internal magnetization $\mathbf{H_0}$ and the H components of the wave field which are normal to $\mathbf{H_0}$ [15]. The tensor permeability for axially (z-axis) biased ferrite microwire can be represented in matrix
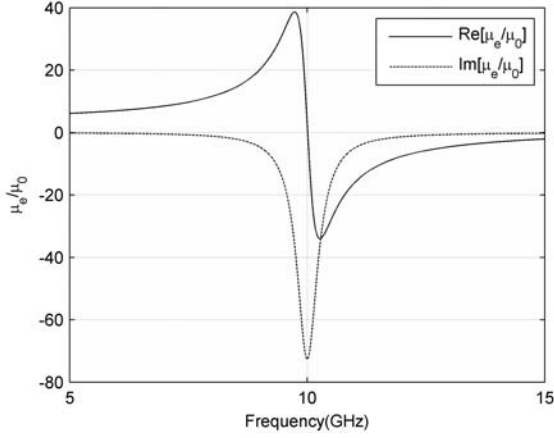
Figure 1: Real and imaginary parts of effective permeability for the considered ferromagnetic microwire (Liberal et al. [8]).
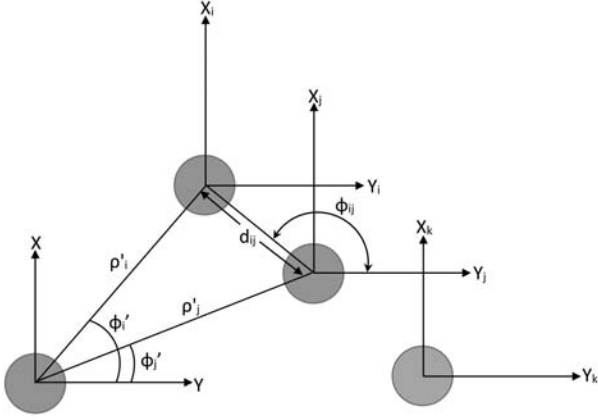

Figure 2: Geometry of the scattering problem.

form as[15]

$$\overline{\overline{\mu}} = \begin{bmatrix} \mu & j\kappa & 0 \\ -j\kappa & \mu & 0 \\ 0 & 0 & \mu_0 \end{bmatrix} \tag{1}$$

where

$$\mu = \mu_0 \left(1 + \chi_p - j\chi_s\right) \tag{2}$$

$$\kappa = \mu_0 \left(K_p - jK_s\right) \tag{3}$$

and

$$\chi_p = \frac{\omega_0\omega_m \left(\omega_0^2 - \omega^2\right) + \omega_0\omega_m\omega^2\alpha^2}{\left[\omega_0^2 - \omega^2 \left(1 + \alpha^2\right)\right]^2 + 4\omega_0^2\omega^2\alpha^2} \tag{4}$$

$$\chi_s = \frac{\omega_0\omega_m\alpha \left[\omega_0^2 + \omega^2 \left(1 + \alpha^2\right)\right]}{\left[\omega_0^2 - \omega^2 \left(1 + \alpha^2\right)\right]^2 + 4\omega_0^2\omega^2\alpha^2} \tag{5}$$

$$K_p = \frac{\omega_0\omega_m\alpha \left[\omega_0^2 - \omega^2 \left(1 + \alpha^2\right)\right]}{\left[\omega_0^2 - \omega^2 \left(1 + \alpha^2\right)\right]^2 + 4\omega_0^2\omega^2\alpha^2} \tag{6}$$

$$K_s = \frac{2\omega_0\omega_m\omega^2\alpha}{\left[\omega_0^2 - \omega^2 \left(1 + \alpha^2\right)\right]^2 + 4\omega_0^2\omega^2\alpha^2}. \tag{7}$$
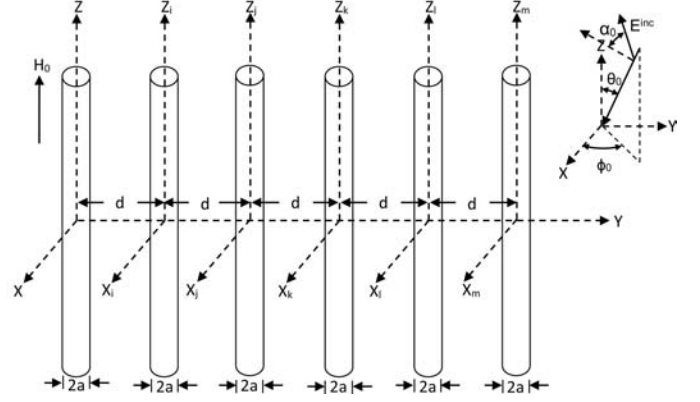

Figure 3: Geometry of the planar array consist of 'M' number of ferromagnetic microwires.

Effective permeability and complex permittivity of the ferrite medium are respectively given by

$$\mu_e = \frac{\mu^2 - \kappa^2}{\mu} \tag{8}$$

$$\epsilon_c = \epsilon_0 - \frac{j\sigma}{\omega}. \tag{9}$$

Let, a finite number of ferrite cylinders of infinite length, each with radius $'a'$ and having applied internal axial magnetization H_0 are placed parallel to each other with their axis along the z-coordinate as shown in Fig.2. Each cylinder is impinged by a uniform plane wave with polarization angle α_0. The z-components of the incident and scattered fields at the surface of the ith cylinder are given in cylindrical coordinates ρ, ϕ and z,respectively by

$$E_{zi}^{inc} = E_0' P_i \cos\alpha_0 \sum_{n=-\infty}^{+\infty} j^n J_n \left(\beta_{\rho_0}\rho\right) e^{-j\beta_z} e^{-jn(\phi_i-\phi_0)}, \tag{10}$$

$$H_{zi}^{inc} = \frac{E_0' P_i}{\eta_0} \sin\alpha_0 \sum_{n=-\infty}^{+\infty} j^n J_n \left(\beta_{\rho_0}\rho\right) e^{-j\beta_z z} e^{-jn(\phi_i-\phi_0)}, \tag{11}$$

$$E_{zi}^s = E_0' \sum_{n=-\infty}^{+\infty} C_n H_n^{(2)}(\beta_{\rho_0}\rho) e^{-j\beta_z z} e^{-jn(\phi_i-\phi_0)}, \tag{12}$$

$$H_{zi}^s = \frac{E_0'}{\eta_0} \sum_{n=-\infty}^{+\infty} D_n H_n^{(2)}(\beta_{\rho_0}\rho) e^{-j\beta_z z} e^{-jn(\phi_i-\phi_0)}. \tag{13}$$

Here $E_0' = E_0 \sin\theta_0, P_i = e^{-j\beta_{\rho_0} \rho_i' cos(\phi_i'-\phi_0)}, \beta_{\rho_0} = \beta_0 \sin\theta_0, \beta_z = \beta_0 \cos\theta_0, \beta_0 = \omega\sqrt{\mu_0\epsilon_0}$, is the free space propagation constant and $\eta_0 = \sqrt{\frac{\mu_0}{\epsilon_0}}$, is the intrinsic impedance of the free space. The superscripts i and s denote the incident and the scattered fields respectively, J_n is the nth order Bessel's function of the first kind, $H_n^{(2)}$ is the nth order Hankel's function of the second kind, C_n and D_n are the unknown expansion coefficients.

The ϕ-components for the incident and scattered fields

9

at the surface of the reference cylinder may be easily deduced from Maxwell's equations to be

$$E_{\phi i}^{inc} = -E_0 P_i \frac{n \cos\theta_0 \cos\alpha_0}{\beta_0 \rho \sin\theta_0} \sum_{n=-\infty}^{+\infty} j^n J_n(\beta_{\rho_0}\rho) e^{-j\beta_z z}$$
$$\times \quad e^{-jn(\phi_i-\phi_0)} + jE_0 \sin\alpha_0 \sum_{n=-\infty}^{+\infty} j^n J_n'(\beta_{\rho_0}\rho)$$
$$\times \quad e^{-j\beta_z z} e^{-jn(\phi_i-\phi_0)}, \tag{14}$$

$$H_{\phi i}^{inc} = -\frac{jE_0 P_i}{\eta_0} \sin\alpha_0 \sum_{n=-\infty}^{+\infty} j^n J_n'(\beta_{\rho_0}\rho)$$
$$\times \quad e^{-j\beta_z z} e^{-jn(\phi_i-\phi_0)} - \frac{E_0}{\eta_0} \frac{n \cos\theta_0 \cos\alpha_0}{\beta_0 \rho \sin\theta_0}$$
$$\times \quad \sum_{n=-\infty}^{+\infty} j^n J_n(\beta_{\rho_0}\rho) e^{-j\beta_z z} e^{-jn(\phi_i-\phi_0)}, \tag{15}$$

$$E_{\phi i}^{s} = -E_0 \frac{n \cos\theta_0}{\beta_0 \rho \sin\theta_0} \sum_{n=-\infty}^{+\infty} C_n H_n^{(2)}(\beta_{\rho_0}\rho) e^{-j\beta_z z} e^{-jn(\phi_i-\phi_0)}$$
$$+ jE_0 \sum_{n=-\infty}^{+\infty} D_n H_n^{(2)'}(\beta_{\rho_0}\rho) e^{-j\beta_z z} e^{-jn(\phi_i-\phi_0)}, \tag{16}$$

$$H_{\phi i}^{s} = -\frac{jE_0}{\eta_0} \sum_{n=-\infty}^{+\infty} C_n H_n^{(2)'}(\beta_{\rho_0}\rho) e^{-\beta_z z} e^{-jn(\phi_i-\phi_0)}$$
$$- \frac{E_0}{\eta_0} \frac{n \cos\theta_0}{\beta_0 \rho \sin\theta_0}$$
$$\times \quad \sum_{n=-\infty}^{+\infty} D_n H_n^{(2)}(\beta_{\rho_0}\rho) e^{-j\beta_z z} e^{-jn(\phi_i-\phi_0)}, \tag{17}$$

where, ' denotes the first derivative with respect to the argument.

The z-components of the inside field for the reference cylinder in cylindrical coordinates ρ, ϕ and z are given by[6, 7],

$$E_{zi}^{d} = E_0 \sum_{n=-\infty}^{+\infty} [A_n J_n(\gamma_{\rho 1}\rho) + B_n J_n(\gamma_{\rho 2}\rho)]$$
$$\times \quad e^{-j\beta_z z} e^{-jn(\phi_i-\phi_0)}, \tag{18}$$

$$H_{zi}^{d} = E_0 \sum_{n=-\infty}^{+\infty} [\eta_1 A_n J_n(\gamma_{\rho 1}\rho) + \eta_2 B_n J_n(\gamma_{\rho 2}\rho)]$$
$$\times \quad e^{-j\beta_z z} e^{-jn(\phi_i-\phi_0)}, \tag{19}$$

$$E_{\phi i}^{d} = E_0 \sum_{n=-\infty}^{+\infty} [A_n X_{1n}(\rho) + B_n X_{2n}(\rho)]$$
$$\times \quad e^{-j\beta_z z} e^{-jn(\phi_i-\phi_0)}, \tag{20}$$

$$H_{\phi i}^{d} = E_0 \sum_{n=-\infty}^{+\infty} [A_n \Lambda_{1n}(\rho) + B_n \Lambda_{2n}(\rho)]$$
$$\times \quad e^{-j\beta_z z} e^{-jn(\phi_i-\phi_0)}, \tag{21}$$

where, $X_{in}(\rho)$ and $\Lambda_{in}(\rho)$ are defined as

$$X_{in}(\rho) = \frac{1}{D}(d\eta_i \gamma_{\rho_i} - b\gamma_{\rho_i}) J_n'(\gamma_{\rho_i}\rho)$$
$$+ \frac{1}{D} \frac{jn(e\eta_i - a)}{\rho} J_n(\gamma_{\rho_i}\rho), \tag{22}$$

$$\Lambda_{in}(\rho) = \frac{1}{D}\left(a\gamma_{\rho_i}\frac{\omega\epsilon_c}{\beta_z} - b\gamma_{\rho_i}\eta_i\right) J_n'(\gamma_{\rho_i}\rho)$$
$$- j\frac{n}{D\rho}\left(a\eta_i + \frac{b\omega\epsilon_c}{\beta_z}\right) J_n(\gamma_{\rho_i}\rho), \tag{23}$$

where

$$a = j\beta_z\beta_\rho^2, \tag{24}$$
$$b = \omega^2\kappa\beta_z\epsilon_c, \tag{25}$$
$$c_1 = \left(\beta_\rho^2 - \frac{\omega^2\kappa^2\epsilon_c}{\mu}\right), \tag{26}$$
$$d = -j\omega\mu c_1, \tag{27}$$
$$e = \omega\kappa\beta_z^2, \tag{28}$$
$$D = (\omega^2\kappa\epsilon_c)^2 - \beta_\rho^4, \tag{29}$$
$$\eta_i = \frac{-jg_1}{(\gamma_{\rho_i}^2 - f_1)}, \tag{30}$$
$$g_1 = \frac{\omega\kappa\beta_z\epsilon_c}{\mu}, \tag{31}$$
$$f_1 = \frac{\mu_0\beta_\rho^2}{\mu}, \tag{32}$$
$$\gamma_{\rho_i} = \sqrt{\frac{1}{2}\left((f_1+c_1) \pm \sqrt{(f_1-c_1)^2+4d_1 g_1}\right)}, \tag{33}$$
$$d_1 = \frac{\mu_0\omega\kappa\beta_z}{\mu}, \tag{34}$$
$$\beta_\rho = \sqrt{(\omega^2\mu\epsilon_c - \beta_z^2)}. \tag{35}$$

Here, i takes the suffix '1' or '2' according to the '+' or '-' sign taken inside the square root in (33), respectively.

In order to calculate the contribution of the other cylinders to total scattered field at the surface of the reference microwire, Graf's theorem is used to transform the scattered field components from one set of coordinates to another[17]. With the help of this theorem, the scattered field of each microwire placed in the vicinity of the reference microwire is transformed in terms of the coordinates of the reference microwire. For example, the scattered field from j^{th} microwire in terms of the ith microwire can be represented as:

$$H_n^{(2)}(\beta_{\rho_0}\rho)e^{jn\phi_g} = \sum_{m=-\infty}^{+\infty} J_m(\beta_{\rho_0}\rho) H_{m-n}^{(2)}(\beta_{\rho_0}d_{ij})$$
$$\times \quad e^{jm\phi_i} e^{j(m-n)\phi_{ij}}, \tag{36}$$

$$d_{ij} = \rho_i'^2 + \rho_j'^2 - 2\rho_i'\rho_j'\cos(\phi_i' - \phi_j') \tag{37}$$

$$\phi_{ij} = \begin{cases} \cos^{-1}\left[\dfrac{\rho_i'\cos(\phi_i') - \rho_j'\cos(\phi_j')}{d_{ij}}\right], \\ for \quad \rho_i'\sin(\phi_i') \geq \rho_j'\sin(\phi_j')' \\ -\cos^{-1}\left[\dfrac{\rho_i'\cos(\phi_i') - \rho_j'\cos(\phi_j')}{d_{ij}}\right], \\ for \quad \rho_i'\sin(\phi_i') < \rho_j'\sin(\phi_j'). \end{cases} \tag{38}$$

The continuity of tangential components of fields at the surface of the ith microwire placed along the z-axis ($\rho = a$)translates to

$$E_{z_i}^{inc} + \sum_{l=1}^{M} E_{z_l}^s = E_{z_i}^d, \tag{39}$$

$$H_{z_i}^{inc} + \sum_{l=1}^{M} H_{z_l}^s = H_{z_i}^d, \tag{40}$$

$$E_{\phi_i}^{inc} + \sum_{l=1}^{M} E_{\phi_l}^s = E_{\phi_i}^d, \tag{41}$$

$$H_{\phi_i}^{inc} + \sum_{l=1}^{M} H_{\phi_l}^s = H_{\phi_i}^d. \tag{42}$$

After substituting the values of the field components form (10) to (21) in (39) to (42) and solving further gives the following equations.

$$\sum_{l=1}^{M} C_{ln}\Theta_{ln} - \sum_{l=1}^{M} D_{ln}\Phi_{ln} = \Psi_{in} \tag{43}$$

$$\sum_{l=1}^{M} C_{ln}\Delta_{ln} - \sum_{l=1}^{M} D_{ln}\Omega_{ln} = \Upsilon_{in} \tag{44}$$

where, $l = 1, 2....M$ is the index number of the cylinders and

$$\Theta_{ln} = \left\{\eta_0\eta_2\sin\theta_0\left(\frac{\chi_{1n}(a)}{U_{1i}} + \frac{\chi_{2n}(a)}{U_{2i}}\right) + \frac{n\cos\theta_0}{\beta_{\rho_0}a}\right\}H_{ln} \tag{45}$$

$$\Phi_{ln} = \left\{\sin\theta_0\left(\frac{\chi_{1n}(a)}{U_{1i}} + \frac{\chi_{2n}(a)}{U_{2i}}\right)H_{ln} + jH_{ln}'\right\}, \tag{46}$$

$$\Psi_{in} = j^n P_i\left\{\sin\alpha J_n'(\beta_{\rho_0}a) - \frac{\cos\alpha\cos\theta_0 J_n(\beta_{\rho_0}a)}{\beta_{\rho_0}a}\right\} \\ - \left(\frac{V_{1i}\chi_{1n}(a)}{U_{1i}} + \frac{V_{2i}\chi_{2n}(a)}{U_{2i}}\right), \tag{47}$$

$$\Delta_{ln} = \left\{\left(\frac{\eta_0\eta_2\Lambda_{1n}(a)}{U_{1i}} + \frac{\eta_0\eta_1\Lambda_{2n}(a)}{U_{2i}}\right)H_{ln} + \frac{jH_{ln}'}{\eta_0}\right\} \tag{48}$$

$$\Omega_{ln} = \left\{\frac{\Lambda_{1n}(a)}{U_{1i}} + \frac{\Lambda_{2n}(a)}{U_{2i}} - \frac{n\cos\theta_0}{\eta_0\beta_{\rho_0}a}\right\}H_{ln}, \tag{49}$$

$$\Upsilon_{in} = j^{n+1}P_i\left\{\cos\alpha J_n'(\beta_{\rho_0}a) + \frac{n\sin\alpha\cos\theta_0 J_n(\beta_{\rho_0}a)}{\beta_{\rho_0}a}\right\} \\ - \left(\frac{V_{1i}\Lambda_{1n}(a)}{U_{1i}} + \frac{V_{2i}\Lambda_{2n}(a)}{U_{2i}}\right), \tag{50}$$

$$U_{1i} = \eta_0(\eta_1 + \eta_2)J_n(\gamma_{\rho1}\rho), \tag{51}$$

$$U_{2i} = \eta_0(\eta_1 + \eta_2)J_n(\gamma_{\rho2}\rho), \tag{52}$$

$$V_{1i} = j^n P_i(\eta_0\eta_2\cos\alpha - \sin\alpha)J_n(\beta_{\rho_0}a), \tag{53}$$

$$V_{2i} = j^n P_i(\eta_0\eta_1\cos\alpha - \sin\alpha)J_n(\beta_{\rho_0}a). \tag{54}$$

η_1 and η_2 are defined as given in [6], and

$$H_{ln} = \begin{cases} H_n^{(2)}(\beta_{\rho_0}\rho), for\, l = i, m = n \\ \sum_{m,n=-\infty}^{+\infty} J_m(\beta_{\rho_0}\rho)\, H_{m-n}^{(2)}(\beta_{\rho_0}d_{ig}), \\ for \quad l \neq i, m = n \\ 0, \quad for \quad m \neq n \end{cases} \tag{55}$$

Here,'m' and 'n' are integers such that $m, n = \pm1, \pm2, ... \pm N_i$ and the value of N_i depends upon the radius $'a_i'$ of the ith cylinder as $N_i \approx (1 + 2k_ia_i)$ where, k_i is the wavenumber of the inside medium of the cylinder. . Similarly, by applying the boundary condition at the surface of each of the 'M' cylinders, all equations are consolidated in the form of a matrix equation as

$$\begin{bmatrix} \Theta & \Phi \\ \Delta & \Omega \end{bmatrix}\begin{bmatrix} C \\ D \end{bmatrix} = \begin{bmatrix} \Psi \\ \Upsilon \end{bmatrix}, \tag{56}$$

The solution of the truncated matrix given by (56) yields the unknown expansion coefficients of the scattered field C_{in} and D_{in}.

Finally, the Scattering cross section is defined as given in [16]

$$\sigma_{2D}^{TM} = 10\log\left[\lim_{\rho\to\infty} 2\pi\rho\frac{|E_z^s|^2}{|E_z^{inc}|^2}\right], \tag{57}$$

and

$$\sigma_{2D}^{TE} = 10\log\left[\lim_{\rho\to\infty} 2\pi\rho\frac{|H_z^s|^2}{|H_z^{inc}|^2}\right]. \tag{58}$$

3. Numerical results

The geometry of the planar array of microwires under consideration is shown in Fig.3. Here, in case of a planar grid, $\phi_{ig} = \pm\pi$ and $d_{ij} = d$, where d is the uniform spacing among the microwires. Since the maximum radius considered is $50\mu m$, radius-to-wavelength ratio at the maximum operating frequency (15 GHz) for the microwire under consideration is only 2.5×10^{-3}. So, the azimuthal dependence of scattered field may be neglected without any significant loss in accuracy. Thus only the term, n = 0 in the expansions for the inside and the scattered field makes the significant contribution. The sample results are obtained for a planar arrays containing six 'Co' based ferrite microwires of the following specifications as considered in [8]: radius, $a = 1\mu m - 50\mu m$, spacing, $d = 3mm$, conductivity, $\sigma = 6.7 \times 10^5 S/m$, gyromagnetic ratio, $\gamma = 2 \times 10^{11}T^{-1}s^{-1}$, saturation magnetization, $\mu_0 M_s = 0.55T$, loss factor, $\delta = 0.02$, internal magnetization, $H_0 = 113.45kA/m$ along the z-coordinate and an operating frequency band of 5-15 GHz is assumed. Simulation results are plotted for the near field distribution in the plane of the array (i.e., $\rho = a$) and scattering cross section (SCS) against the operating frequency radius of the microwires, spacing among the microwires and the incident angle θ_0 for two different polarization angles, $\alpha_0 = 0°$ and $90°$(i.e.,TM_z and TE_z polarizations respectively).
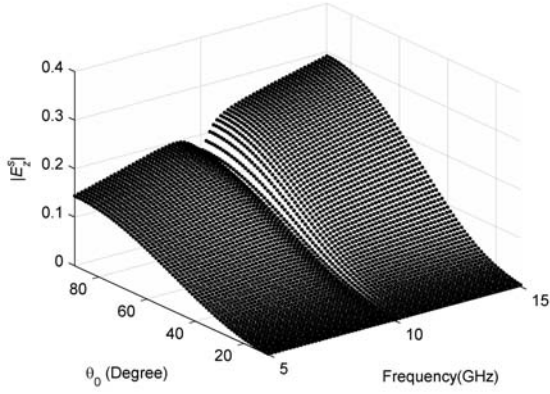
Figure 4: Near field component of the array consist of 6 ferromagnetic microwires at $\phi_i = 0^o$(y-z plane) for TM_z Polarization.
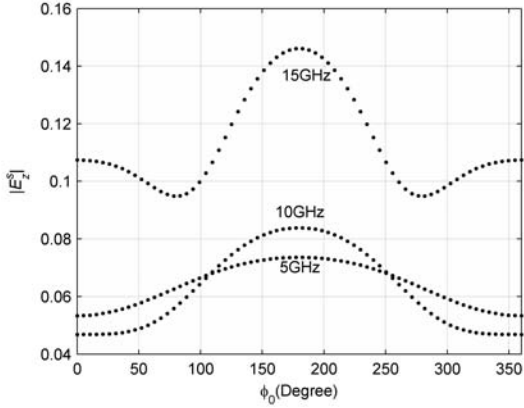

Figure 5: Near field distribution in the x-y plane for the array consist of 6 ferromagnetic microwires for TM_z Polarization at 15 GHz, 10 GHz and 5 GHz at $\theta_0 = 45°$ and $\phi_i = 0^o$.

3.1. TM_z **Polarization (i.e., $\alpha_0 = 0°$)**

3.1.1. Near Field

Fig.4 shows the numerical results of near field component of the scattered field calculated in the plane of the array (i.e., $\rho = a$) plotted against the incident angle θ_0 and operating frequency .The scattering behavior of the grid is may conveniently be explained with the help of the scattering behavior of the single microwire as explained in [4] in terms of two frequency-ranges containing frequencies below and above FMR(i.e., 10GHz) where $Re[\mu_e] > 0$ and $Re[\mu_e] < 0$, respectively(see in Fig.1). For frequencies below FMR,$Re[\mu_e] > 0$ as shown in in Fig.1, the medium inside the microwire behaves similar to lossy dielectric and thus the scattering is weak. However, for frequencies above FMR, $Re[\mu_e] < 0$. As a result, the imaginary part of the propagation constant(phase constant) of ferrite medium becomes negative. Consequently, the microwire supports only evanescent field inside and the microwire essentially be-
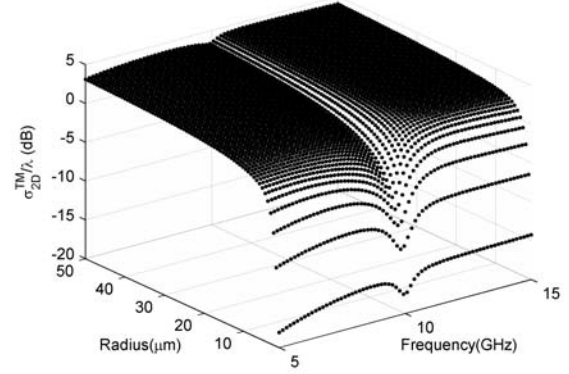

Figure 6: Scattering cross section (SCS) of an array consist of 6 ferromagnetic microwires plotted for TM_z polarization against the frequency and radius of the microwires at $\theta_0 = 45°$ and $\phi_i = 0^o$.
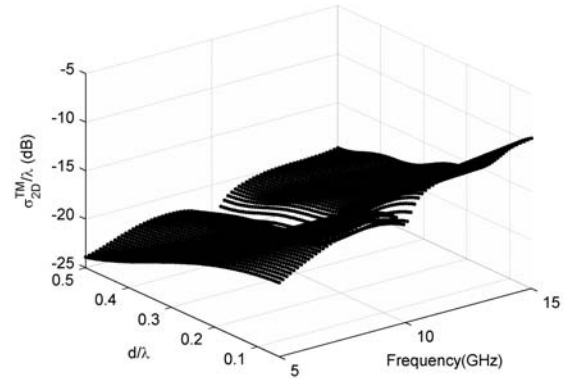

Figure 7: Scattering cross section (SCS) of an array consist of 6 ferromagnetic microwires plotted for TM_z polarization against the frequency and spacing 'd' among the microwires at $\theta_0 = 45°$and $\phi_i = 0^o$.

haves like a plasma region giving rise to increased scattering. In other words, there is a remarkable difference in the scattering behavior of the single microwire for the frequencies below and above FMR. The magnitude of the near field for small angle of incidence(say $\theta_0 \rightarrow 10°$) turns out to be very small because of the low values of the tangential field components.

Fig.5 shows the distribution of the near field in the x-y plane plotted at three different frequencies (i.e., 15 GHz, 10GHz and 5 GHz respectively) for a planar array containing six ferromagnetic microwires each of radius $1\mu m$ (see in Fig.3). It can be seen in Fig. 5 that maximum scattering takes place for $\phi_0 = 180^o$ i.e., backscattering is more dominant.

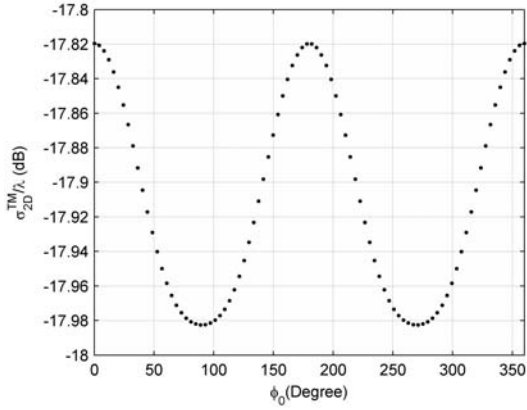Figure 8: Scattering cross section (SCS) of an array consist of 6 ferromagnetic microwires at 10 GHz for TM_z Polarization and $\theta_0 = 45°$, $\phi_i = 0^o$.
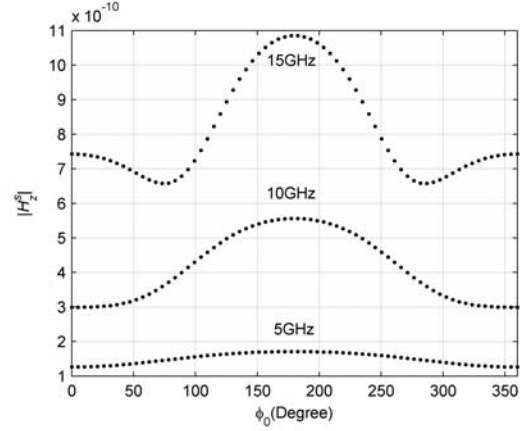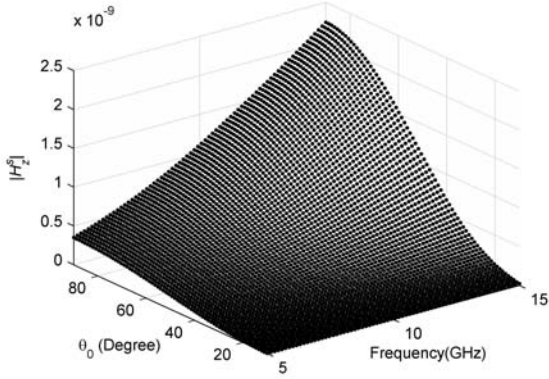

Figure 10: Near field distribution in the x-y plane for the array consist of 6 ferromagnetic microwires for TE_z Polarization at 15 GHz, 10 GHz and 5 GHz at $\theta_0 = 45°$ and $\phi_i = 0^o$.

Figure 9: Near field component of the array consist of 6 ferromagnetic microwires at $\phi_i = 0^o$ (y-z plane) for TE_z Polarization.
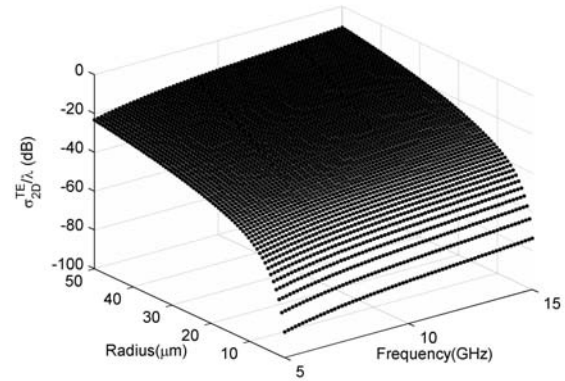

Figure 11: Scattering cross section (SCS) of an array consist of 6 ferromagnetic microwires plotted for TE_z polarization against the frequency and radius of the microwires at $\theta_0 = 45°$, $\phi_i = 0^o$.

3.1.2. Scattering Cross section

Fig.6 and Fig.7 shows the numerical results of Scattering Cross section (SCS) for a planar array containing six ferromagnetic microwires each of radius $1\mu m$ (see in Fig.3). In Fig.6, SCS is plotted against the radius of the microwires and operating frequency. It can be seen in Fig.6, as the radius increases from $1\mu m$ to $10\mu m$, there is about 20 dB rise in the magnitude of SCS while beyond $10\mu m$, the SCS increases by 4 dB only. This is on account of the increment in the magnitude of scattered field from thicker microwires. In Fig.7, SCS is plotted against the spacing among the microwires 'd' and operating frequency. It is to be noticed from Fig.7 that the magnitude of SCS decreases as the spacing among the microwire reaches closer to the operating wavelength.

In Fig.8, SCS is plotted at 10 GHz and incident angle $\theta_0 = 45^o, \phi_i = 0^o$. It can be noticed from Fig.8 that the magnitude of SCS varies negligibly (0.16 dB only) around the entire x-y plane with maximum at $\phi_0 = 0^o, 180^o, 360^o$

and minimum at $\phi_0 = 90^o, 270^o$.

3.2. TE_z Polarization (i.e., $\alpha_0 = 90°$)

3.2.1. Near Field

Fig.9 shows the numerical results of near field component of the scattered field calculated calculated in the plane of the array plotted against the incident angle θ_0 and operating frequency for a planar array containing six ferromagnetic microwires each of radius $1\mu m$(see in Fig.3). In this case, there is no interaction of applied internal magnetization **H₀** and the H components of the wave field as the **H** vector of the incident wave is in a plane along the wire(i.e., z-axis)i.e, parallel to the internal magnetization. Hence, there is no effect of ferromagnetic resonance observed and an ordinary wave propagation takes place inside the ferrite medium. Consequently, the ferrite medium behaves like a lossy dielectric medium which results in a very weak scat-
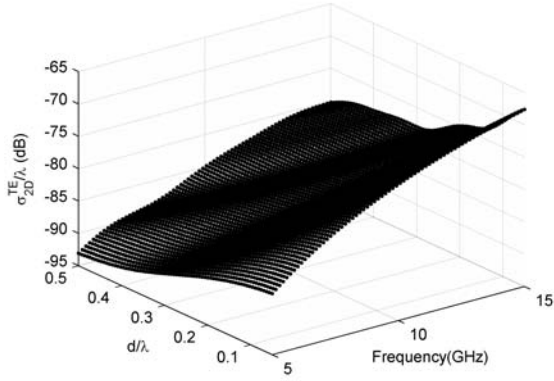
Figure 12: Scattering cross section (SCS) of an array consist of 6 ferromagnetic microwires plotted for TE_z polarization against the frequency and spacing 'd' among the microwires at $\theta_0 = 45°$, $\phi_i = 0°$.
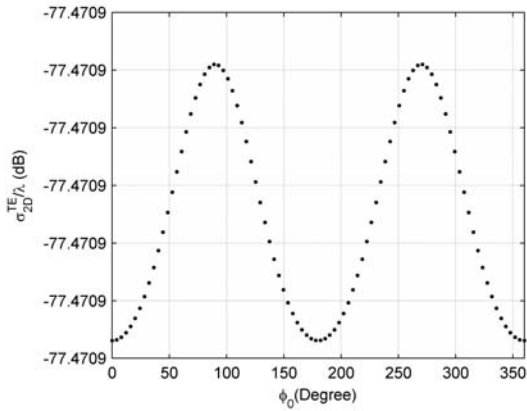

Figure 13: Scattering cross section (SCS) of an array consist of 6 ferromagnetic microwires at 10 GHz for TE_z Polarization and $\theta_0 = 45°$, $\phi_i = 0°$.

Figure 14: Comparison of the Scattering cross section (SCS) of an array consist of 6 ferromagnetic microwires with an array consist of 3 ferromagnetic microwires at 10 GHz for TM_z Polarization and $\theta_0 = 45°$, $\phi_i = 0°$.

Figure 15: Comparison of the Scattering cross section (SCS) of an array consist of 6 ferromagnetic microwires with an array consist of 3 ferromagnetic microwires at 10 GHz for TE_z Polarization and $\theta_0 = 45°$, $\phi_i = 0°$..

tered field. Further, it can be seen in Fig.9, the magnitude of the scattered field increases with frequency. This is because, the skin depth decreases with an increment in frequency and as a results in the decrement in the Transmitted field is compensated by the increment in the magnitude of the scattered field.

Fig.10 shows the distribution of the near field in the x-y plane at three different frequencies (i.e., 15 GHz, 10GHz and 5 GHz respectively)for a planar array consist of six ferromagnetic microwires each of radius $1\mu m$ (see in Fig.3). It can be seen in Fig. 10 that maximum scattering takes place for $\phi_0 = 180°$ i.e., backscattering is more dominant just like the case of TM_z polarization.

3.2.2. Scattering Cross section

Fig.11 and Fig.12 shows the numerical results of Scattering Cross section (SCS) for a planar array containing six ferromagnetic microwires each of radius $1\mu m$ (see in Fig.3). In
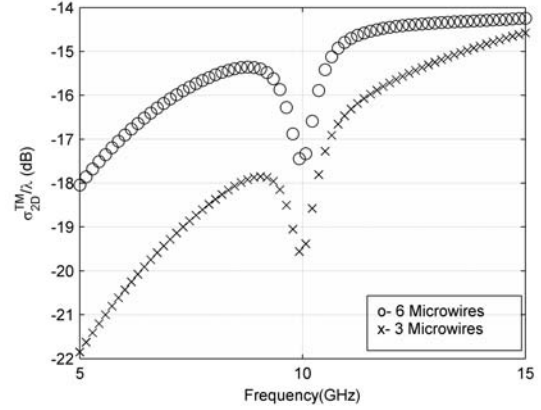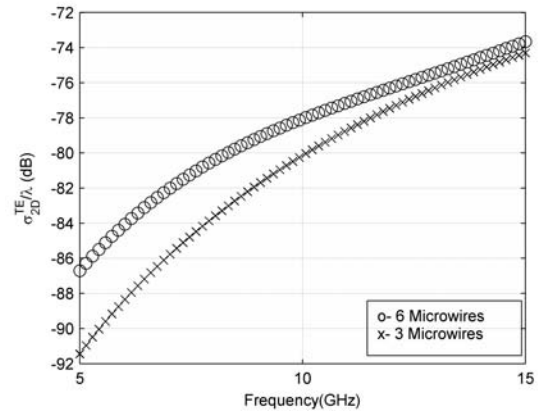
Fig.11, SCS is plotted against the radius of the microwires and operating frequency. Both kind of plots are characterized by the absence of FMR(Ferromagnetic resonance) as discussed earlier. It can be seen in Fig.11, as the radius increases from $1\mu m$ to $10\mu m$, there is about 50 dB rise in the magnitude of SCS while beyond $10\mu m$, the SCS increases only about 20 dB. Once again, this is on account of the increment in the magnitude of scattered field from thicker microwires. In Fig.12, SCS is plotted against the spacing among the microwires 'd' and operating frequency. Similar to the TM_z case, the magnitude of SCS decreases as the spacing among the microwire reaches closer to the operating wavelength.

In Fig.13, SCS is plotted at 10 GHz and incident angle $\theta_0 = 45°$, $\phi_i = 0°$. It can be noticed from Fig.10 that the magnitude of SCS varies negligibly around the entire x-y plane. It represents an almost uniform SCS in the x-y plane. This is due to the fact that each microwire has a ra-
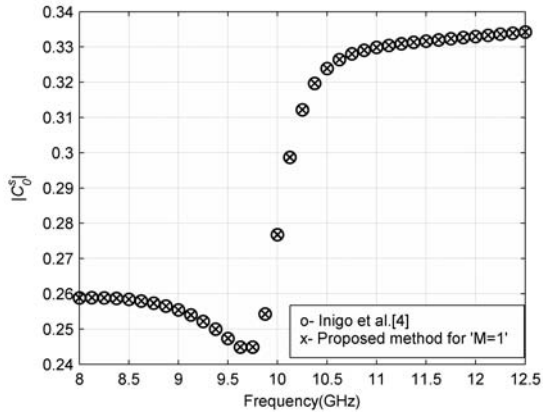
Figure 16: Comparison of the results of scattering field coefficient specialized to the case of $\theta_0 = 90^o$ and 'M=1' for TM_z Polarization (i.e. normal incidence and single ferromagnetic microwire) with the result available in [4] for the specialized case.
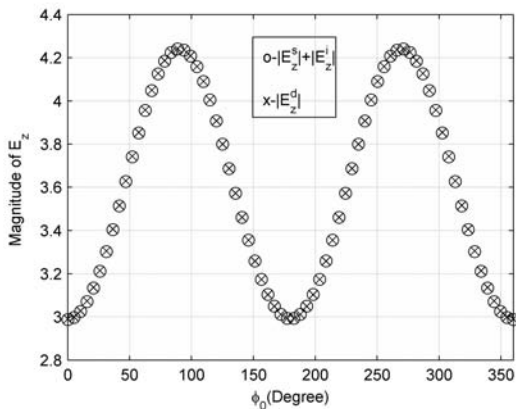

Figure 17: Continuity of the E_z for TM_z Polarization.

dius $1\mu m$ which is much less than the wavelength. Hence, the azimuthal dependence of the scattered field of an individual microwire was neglected..

3.3. Comparison of the results

Fig.14 and Fig.15 shows the comparison of the Scattering cross section (SCS) of an array of 6 microwires with an array of 3 microwires each of radius $1\mu m$ for TM_z and TE_z Polarizations receptively at $\theta_0 = 45°$. It clearly shows the rise in magnitude of SCS as the number of microwires increase in both cases.

Fig.16 shows a comparison of the results for the expansion coefficient of the scattered field C_0^s, of order zero as given in [4] for single microwire at normal incidence and TM_z Polarization characterized by the following parameters: radius, $a = 45\mu m$, conductivity, $\sigma = 6.5 \times 10^4 S/m$, gyromagnetic ratio, $\gamma = 1.33 \times 10^{11} T^{-1} s^{-1}$, saturation magnetization, $\mu_0 M_s = 0.55T$, loss factor, $\delta = 0.02$, internal magnetization, $H_0 = 213kA/m$ along the z-coordinate
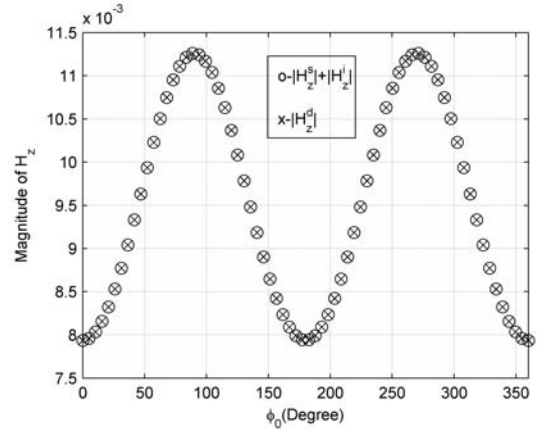

Figure 18: Continuity of the H_z for TE_z Polarization.

and an operating frequency band of 8-12 GHz. with the results obtained by substituting $'M = 1'$, $\alpha_0 = 0°$ and $\theta_0 = 90°$ in (56). As we can see, results of the proposed analysis for this specialized case reduce to the results available in [4].

3.4. Continuity of the Fields

Finally, continuity of the tangential field components considered in this analysis is proved with the help of Fig.17 and Fig.18 for E_z and H_z components, respectively. In Fig.17, $|E_z^s| + |E_z^i|$ (z-components of the incident and scattered fields) and $|E_z^d|$ (z-component of the inside field) are shown to be matched perfectly at the surface of reference microwire for TM_z polarization. Similarly, Fig.18 shows the matching of the $|H_z^s| + |H_z^i|$ (z-components of the incident and scattered fields) and $|H_z^d|$ (z-component of the inside field) for TE_z polarization.

4. Conclusion

A boundary value type solution for the generalized case of scattering from an array consist of a finite number of ferrite cylinders is presented in this paper. The derivation was carried out by using the tangential boundary conditions at the surface of each microwire in order to find the unknown expansion coefficients of the scattered field. Proposed method took less efforts as there was no need to re-derive the inside field expressions and already available expressions were utilized to derive the final results. Effect of the radius of microwires, relative spacing among the microwires and incident angle upon the scattering behavior of the array was presented with a numerical example of a planar arrays containing six microwires. Numerical results are expressed in terms of the near field components and Scattering cross section (SCS) for TM_z and TE_z polarizations respectively. It is shown here that the case of electromagnetic scattering from single ferromagnetic microwire available in the literature, is a special case of the proposed analysis. Authors expect that the present analysis may find many application including wire based metamaterials.

References

[1] Louis-Philippe Carignan, Arthur Yelon and David Ménard, "Ferromagnetic Nanowire Metamaterials: Theory and Applications", IEEE Trans Microwave Theory Techn,vol. 59,no.10,pp. 2568-2586,Oct.2011, DOI: 10.1109/TMTT.2011.2163202.

[2] J. Carbonell, H. G. Miqule, and J. S. Dehsa,"Double Negative Metamaterials Based on Ferromagnetic Microwires ", Physical Review B,vol. 81, pp. 024401, 2010.

[3] J. Pendry, A. Holden, W. Stewart, and I. Youngs, "Extremely low frequency plasmons in metallic mesostructures", Phys. Rev. Lett., vol. 76, no. 25, pp. 47734776, 1996.

[4] Liberal Iñigo, Ederra Iñigo, Gómez-Polo Cristina, Labrador Alberto, Pérez Landazábal Jose Ignacio and Gonzalo Ramón,"Theoretical Modeling and Experimental Verification of the Scattering From a Ferromagnetic Microwire", IEEE Trans Microwave Theory Techn, vol.59, no.3,pp.517-526, Mar. 2011, DOI: 10.1109/TMTT.2010.2098037

[5] W. H. Eggimann, "Scattering of a Plane Wave on a Ferrite Cylinder at Normal Incidence", IEEE Trans Microwave Theory Techn vol. 8, no. 4, pp 440-445,Jul. 1960, DOI: 10.1109/TMTT.1960.1124754.

[6] Ahmed M. Attiya and Majeed A. Alkanhal,"Generalized Formulation for the Scattering from a Ferromagnetic Microwire ", ACES Journal, vol. 27, No. 5, May 2012.

[7] R. A. Waldron, "Electromagnetic Wave Propagation in Cylindrical Waveguides Containing Gyromagnetic Media ", Journal of the British Institution of Radio Engineers, vol.18, no.10, pp.597-612, Oct. 1958.

[8] I. Liberal, I. S. Nefedov, I. Ederra, R. Gonzalo, and S. A. Tretyakov, "Electromagnetic Response and Homogenization of Grids of Ferromagnetic Microwires", J. Appl. Phys., vol. 110, pp. 064909,2011

[9] T. Kumar, N. Kalyanasundaram, and B. K. Lande,"Analysis of the generalized case of scattering from a ferromagnetic microwire grid ", Progress In Electromagnetics Research M, Vol. 35, 1-10, 2014. doi:10.2528/PIERM13120406

[10] M. Polewski and J. Mazur, "Scattering by an array of conducting, Lossy Dielectric, Ferrite and Pseudochiral Cylinders ", Progress In Electromagnetics Research, PIER 38, 283310, 2002.

[11] Atef Z. Elsherbeni, "A comparative study of the two dimensional multiple scattering technique ", Radio science, Vol.24, No. 4, pp.1023-1033, Jul-Aug. 1994.

[12] Christos G. Christodoulou and J. Frank Kauffman,"On the Electromagnetic Scattering from Infinite Rectangular Grids with Finite Conductivity", IEEE Trans. on Antenna and Propg., Vol. AP-34, No. 2, Feb. 1986.

[13] B. H. Henin, A. Z. Elsherbeni, and M. Al Sharkawy "Oblique incidence of plane wave scattering from an array of circular dielectric cylinders", Progress In Electromagnetics Research, PIER 68, 261279, 2007.

[14] N. Okamoto, "Scattering of Obliquely Incident Plane wave from a finite periodic structure of ferrite cylinders", IEEE Trans. on Antenna and Propg., Vol.AP-27, No.3, 317-323, 1979.

[15] D. M. Pozar, "Microwave Engineering", New York: Wiley, 4th edition, 2012, Chapter 9.

[16] C. A. Balanis, "Advanced Engineering Electromagnetics", John Wiley and Sons, 2nd edition, 2012,Chapter 11.

[17] M. Abramowitz and I. Stegun, "Handbook of Mathematical Functions", Dover, 1965.